

ENVIRONMENTAL MEASUREMENTS LABORATORY

EML-619



Comparison of NaI and HPGe Minimum Detectable Activities



Paul Bailey

January 2003

201 Varick Street, 5th Floor, New York, NY 10014-4811
<http://www.eml.doe.gov>

COMPARISON OF NAI AND HPGE MINIMUM DETECTABLE ACTIVITIES

Paul Bailey

**Environmental Measurements Laboratory
U.S. Department of Energy
201 Varick Street, 5th Floor
New York, NY 10014-4811**

November 2002

DISCLAIMER

“This report was prepared as an account of work sponsored by an agency of the United States Government. Neither the United States Government nor any agency thereof, nor any of their employees, makes any warranty, express or implied, or assumes any legal liability nor responsibility for the accuracy, completeness, or usefulness of any information, apparatus, product, or process disclosed, or represents that its use would not infringe privately owned rights. Reference herein to any specific commercial product, process or service by trade name, trademark, manufacturer, or otherwise, does not necessarily constitute or imply its endorsement, recommendation, or favoring by the United States Government or any agency thereof. The views and opinions of authors expressed herein do not necessarily state or reflect those of the United States Government or any agency thereof.”

This report has been reproduced directly from the best available copy.

Available to DOE and DOE Contractors from the Office of Scientific and Technology Information, P.O. Box 62, Oak Ridge, TN 37831; prices available from (423) 576-8401.

Available to the public from the U.S. Department of Commerce, Technology Administration, National Technical Information Service, 5285 Port Royal Road, Springfield, Virginia 22161, (703) 487-4650.

ABSTRACT

The Minimum Detectable Activity of a 76 mm by 76 mm (3" by 3") sodium iodide (NaI) crystal and 18 %, 42 % and 68 % efficient HPGe detectors were calculated and compared for gamma-ray spectrometry with count times in the range of 1 second to 15 minutes. All cases were for *in situ* measurements with a surface distribution source and a detector height of 1 meter. The radionuclides considered were ^{137}Cs and ^{60}Co .

TABLE OF CONTENTS

Introduction.....	1
Methods	1
Results	6
Discussion	6
Acknowledgements.....	7
References	8
Tables	9-11
Figures	12-16
Appendix A.....	17

INTRODUCTION

Effective interdiction of radioactive materials across busy portals will require rapid sampling by robust systems. In many cases, initial screening monitors will have only a few seconds to determine if a specific unit should be further inspected. Consequence management may also require short sample times to rapidly identify materials involved in an event or even to determine if an event has occurred. These applications of radiation monitoring systems require a reevaluation of existing detector technology to determine their merit for addressing these new challenges.

This report specifically addresses the Minimum Detectable Activity (MDA) of the two high efficiency gamma-ray spectroscopy systems, Hyper Pure Germanium (HPGe) detectors and sodium iodide (NaI) detectors. While HPGe detector systems are often considered to be more sensitive due to their superior energy resolution (narrower peak shape), this report quantifies how well this resolution translates into MDA improvements. It is important to note that since the HPGe detectors are significantly more expensive (Table 1), require cooling to ~90 K, and have more frequent catastrophic failures, it is not enough to simply say that HPGe systems are “better” than NaI systems.

In addition, the NaI crystal is distinguished from the HPGe detectors in that the peaks are so broad that counts from one energy may interfere significantly with counts from another energy several tens of keV away. However, data quality objectives may or may not require the ability to resolve low levels of one radioactive nuclide when another is present (i.e. for interdiction, simply detecting the presence of any isotope of concern is the primary goal).

METHODS

DETECTORS

The detectors considered include a 76 mm by 76 mm (3" by 3") NaI and three HPGe detectors with relative efficiencies of 18 %, 42 %, and 68 %.

SOURCES

While, in general, the count rate in any given group of channels in a detector system is a function of background as well as scattered counts (i.e. the MDA will increase as the level of other isotopes with higher energy gammas increases), this report considers only the MDAs for spectra containing only ^{137}Cs or ^{60}Co .

SOURCE GEOMETRY

The geometry used in the calculations is an infinite plane source because this is close to the source distribution of a fallout event and this geometry has a significant fraction (~2/3 at 1 MeV) of the fluence from points between 80° and 90° from the detector's zenith (θ on Figure 1). As such, this geometry is similar to horizontally displaced sources and, to a lesser extent, an immersion cloud.

COUNT TIME

Some applications of these detectors have samples that are only near the detector for a few seconds, as in the case of a moving source or a moving detector. In other applications, the count times are dictated by the data quality objectives and by the amount of time the user has to wait for the sampling to end, for example when using gamma ray spectroscopy for radiation surveys to support environmental remediation. The count time may also be dictated by temporal resolution requirements, as in long term environmental monitoring. Because of these considerations, several count times were considered.

MINIMUM DETECTABLE ACTIVITY CALCULATION

The MDA of a detector was defined by Strom and Stansbury (1993)

$$MDA \equiv \frac{3 + 3.27 \cdot \sqrt{B \cdot t_s (1 + t_s / t_b)}}{eff \cdot t_s} \quad (1)$$

where B is the background count rate¹ in the setting of interest, t_s is the count time of the sample, t_b is the count time of the background, and eff is the efficiency of the detector.

¹ This analysis regards a single isotope. Thus, contrary to conventional gamma-ray spectrum analysis, the number of counts under a peak of interest can be measured in a background spectrum, and need not be estimated using the continuum.

This formula has the advantage of allowing longer background count times than sample count times. When placing a detector in a location for real time monitoring or interdiction, there is often plenty of time to take a background spectrum, so $t_b \gg t_s$ and the t_s/t_b term goes to zero

$$\lim_{t_s/t_b \rightarrow 0} (MDA) = \frac{3 + 3.27 \cdot \sqrt{B \cdot t_s}}{eff \cdot t_s} \quad (2)$$

However, the more conservative assumption that the background count rate is measured for the same amount of time as the sample count rate may also be of interest (i.e. $t_b = t_s$) and the conservative MDA_c can be defined as²

$$MDA_c \equiv \frac{3 + 4.62 \cdot \sqrt{B t_s}}{eff \cdot t_s} \quad (3)$$

Both of these situations will be considered in this paper.

EFFICIENCY CALCULATION

In this context, the efficiency (eff) is taken to be the conversion factor for *in situ* spectrometry as described in IRCU Report 53, Equation 3.1, for an infinite plane source geometry.

$$eff = \frac{\dot{N}}{A_x} = \frac{\dot{N}}{\dot{N}_0} \cdot \frac{\dot{N}_0}{\phi} \cdot \frac{\phi}{A_x} \quad (4)$$

where \dot{N}/A_x is the detector's full absorption peak count rate per unit activity from the nuclide of interest in the geometry of interest; \dot{N}/\dot{N}_0 is the detector and geometry dependent term to correct for the angular response of the detector; \dot{N}_0/ϕ is the detector dependent full absorption peak count rate from plane parallel incident fluence from the nuclide of interest; and ϕ/A_x is the geometry dependent uncollided fluence rate per unit source activity. Since each detector's angular response is a function of that particular detector's physical shape and there is no "standard" shape for the HPGe detectors, all

detectors' angular response term (\dot{N}/\dot{N}_0) were set to unity to generalize the results of this report beyond the specific detector shapes available to EML.³ Each detector's response to plane parallel flux (\dot{N}_0/ϕ) was measured using a point source at 1m or more normal to the detector face (Table 2). The fluence rate term (ϕ/A_x) was calculated numerically using very fine Euler integration (0.02 degrees per step) using Finck's (1992) Equation 2.9

$$\Phi = \int_0^{90} \left(\frac{A_{area}}{2} \right) \cdot \tan(\theta) \cdot \exp(-\mu_{air} \cdot h \cdot \sec(\theta)) \quad (5)$$

where θ is the zenith angle to the point of interest (Figure 1); A_{area} is the activity per unit area, μ_{air} is the air attenuation coefficient at the energy of interest; and h is the height of the detector above the ground.

For a given detector, the efficiency is a function of the nuclide since \dot{N}/\dot{N}_0 and μ_{air} are functions of the nuclide's gamma emission spectrum, so MDA calculations must be carried out on a nuclide by nuclide basis with a separate efficiency calculation for each nuclide.

BACKGROUND COUNT RATE

In order for MDAs to be comparable, they need to regard the MDA in the same sampling environment. For this paper, the setting of interest was the roof of the penthouse of 201 Varick St., New York. This choice is arbitrary, but it is notable that spectra taken on the roof are qualitatively similar to the spectra of backgrounds taken *in situ* over an uncontaminated soil.⁴ The background was measured on the roof of the penthouse exclusively with the NaI detector. Thus the backgrounds for the HPGe detectors, which were collected over soil or the main roof, must be normalized to the roof penthouse using

² Note that MDA_c is also applicable when measuring gamma-ray count rates conventionally, and estimating the background using an estimate of the continuum at both sides of the full energy peak.

³ Experience with HPGe detectors of various shapes indicates values of \dot{N}/\dot{N}_0 are generally within 35% of unity.

⁴ Here "qualitatively similar" is used because the primary nuclides present are the ²³⁸U series, the ²³²Th series, and ⁴⁰K, and the scattering environment is similar in that concrete/brick have essentially the same mass attenuation coefficients as soil in the energy range of interest (0.1 to 3MeV).

$$B \equiv B_{roof} \approx B_s \cdot \frac{X_{roof}}{X_s} \quad (6)$$

here X_{roof}/X_s is a correction factor on the B_s term, where B_s is the background count rate measured over soil (Table 2); X_{roof} is the exposure rate due to gammas on the roof of the penthouse of 201 Varick St. and X_s is the exposure rate where the background reading was taken. This approximation assumes that a change in the exposure rate will be reflected by a proportional change in the count rate in the regions of interest for ^{60}Co and ^{137}Cs . Assuming that the only significant contribution to the gamma radiation field and exposure rate are from the ^{238}U series, the ^{232}Th series, and ^{40}K and all these sources have gammas above the 1.3 MeV gamma in ^{60}Co , any increase in the exposure rate will also lead to an increase in the background count rate of the detector in all the regions of interest (all of which are within 650-1340 keV). The approximation is also helped by the fact that the higher energy gammas are more heavily weighted in the exposure rate calculation. Given the amount of information available, and the observation that the spectra are qualitatively similar, this is probably the best correction given the data. Note that the correction factors (X_{roof}/X_s) are close to unity, and the largest correction is 26 % of the measured quantity B_s , i.e.

$$\max(\text{abs}(1 - X_{roof}/X_s)) = 0.26 \quad (7)$$

The exposure rate was calculated for the HPGe measurements using EML standard *in situ* spectrometry techniques for Ge detectors (Beck et al. 1972). The background exposure rate due to gammas on the roof of the penthouse at 201 Varick St. was measured using a pressurized ionization chamber, assuming a contribution of 3.6 $\mu\text{R}/\text{h}$ from secondary cosmic radiation at an outdoor location near sea level (Bouville and Lowder, 1988).⁵

⁵ The conversion from $\mu\text{Sv y}^{-1}$ (as reported by Bouville and Lowder) to $\mu\text{rad hr}^{-1}$ is trivial given their assumption of a quality factor of unity. The conversion from Rad to Roentgen is nonstandard in that Roentgen is normally not defined for energies above 3 MeV. However, this use of Roentgen to describe cosmic radiation follows Miller and Beck (1984) who refer to it as the “exposure rate equivalent of ionization due to cosmic rays.”

RESULTS

The resulting MDAs and MDA_cs in Bq cm⁻² at select times are presented for ¹³⁷Cs (Table 3) and ⁶⁰Co (Table 4). The MDAs were plotted relative to the MDAs of the NaI for ¹³⁷Cs (Figure 2) and ⁶⁰Co (Figure 3) and MDA_cs for ¹³⁷Cs (Figure 4) and ⁶⁰Co (Figure 5). All HPGe values can be compared to the NaI values with a 12 % relative uncertainty level (Appendix A).

DISCUSSION

The performance of the NaI detector was proportionally better at small count times. In fact, the NaI outperformed the 18 % efficient HPGe below a few seconds sampling time. The NaI detector is more efficient and thus gets more counts in its Regions of Interest (ROIs), giving it the relative advantage of quickly achieving enough counts to separate counts due to nuclides of interest from counts due to background. However, this effect becomes less and less important as the count time increases and the background is well sampled enough that it is out of the noise of very small counting statistics.

The absolute MDA was always less than the MDA_c, highlighting the advantage of a long background sample time. In the comparisons the HPGe detectors performed relatively better under the conservative assumption that the background was counted for the same amount of time as the sample. For the HPGe detector, the constant term in the numerator is the dominant term at short count times while for the NaI detector the second term is always dominant. This can be attributed to NaI detectors' relatively broad peaks leading to large ROIs and thus larger background count rates relative to its efficiency, giving it a relatively larger MDA as compared to a similar efficiency HPGe detector.

For a 1 second count time the NaI was not outperformed by significantly more than a factor of 2 by any of the HPGe detectors.

Inspection of (Equation 1) shows that at large count times (once the first term in the numerator has an insignificant contribution), the ratio of the MDA equations will level off at a constant value. At large count times, the MDA and MDA_cs of the HPGe detectors leveled off at about 2 times lower than the NaI for the 18 % efficient HPGe detector, 3

times lower than the NaI for the 42 % efficient HPGe detector, and 5 times lower than the NaI for the 68 % efficient HPGe detector.

ACKNOWLEDGMENTS

The author would like to thank C. V. Gogolak for assistance with the Appendix and K. M. Miller for the HPGe data and many valuable discussions.

REFERENCES

Beck, H., J. De Campo, and C. Gogolak

In Situ Ge(Li) and NaI(Tl) Gamma-Ray Spectrometry.

U.S. Atomic Energy Commission Report HASL-258, New York, NY (1972)

Bouville, A. and W. Lowder

Human Population Exposure to Cosmic Radiation

Radiation Protection Dosimetry 24:293-299 (1988)

Finck R.

Field Gamma Spectrometry: and its Application to Problems in Environmental Radiology

Ph.D. Dissertation, Lund University, ISBN 91-628-0739-0, Malmö and Lund Sweden (1992)

International Commission on Radiation Units and Measurements (ICRU)

Gamma-ray Spectrometry in the Environment

ICRU Publication 53, Bethesda, Maryland (1994)

Miller, K. and H. Beck

Indoor Gamma and Cosmic Ray Exposure Rate Measurements Using a Ge Spectrometer
and Pressurised Ionisation Chamber

Radiation Protection Dosimetry 7:185:189 (1984)

Strom, D. J. and P. S. Stansbury

Minimum Detectable Activity When Background is Counted Longer than the Sample

Health Physics 63:360-361 (1993)

Table 1. Gamma-ray detector costs.

detector	cost ³
76 mm x 76 mm NaI	\$1,100
20 % HPGe	\$16,000
40 % HPGe	\$26,000
65 % HPGe	\$42,000

³all costs from an estimate in 2002 and are reported to two significant figures.

Table 2. Background measurement and efficiency data.

detector	location	X _s exposure rate (μR h ⁻¹)	¹³⁷ Cs efficiency (s ⁻¹ per Bq cm ⁻²)	¹³⁷ Cs peak width (keV)	B _s ¹³⁷ Cs background count rate (s ⁻¹)	⁶⁰ Co efficiency (s ⁻¹ per Bq cm ⁻²)	⁶⁰ Co peak width (keV) ^c	B _s ⁶⁰ Co background count rate (s ⁻¹)
NaI	EML roof, penthouse	3.5 ^a	31.8	120	5.851	53.6	300	4.553
18 % HPGe	EML roof, main	4.6 ^b	6.7	3	0.030	10.7	6	0.025
42 % HPGe	Kings Park, NY	3.3 ^b	14.4	3	0.074	25.9	6	0.062
68 % HPGe	Upton, NY	4.2 ^b	21.6	3	0.113	37.9	6	0.074

^aMeasured by pressurized ionization chamber, excludes cosmic contribution assumed to be equivalent to 3.6 μR/h.

^bCalculated using spectral stripping.

^cAll ⁶⁰Co data includes both peaks.

Table 3. Selected MDA and MDA_c values for ¹³⁷Cs.

t _s (s)	t _b (s)	MDA _c (eq 3) (Bq cm ⁻²)			
		NaI	18 %	42 %	68 %
1	1	0.45	0.57	0.30	0.21
10	10	0.12	0.083	0.049	0.037
60	60	0.047	0.023	0.015	0.012
900	900	0.015	0.0057	0.0039	0.0032
		MDA (eq 2) (Bq cm ⁻²)			
1	∞	0.34	0.53	0.15	0.19
10	∞	0.088	0.072	0.0215	0.030
60	∞	0.034	0.018	0.0060	0.0089
900	∞	0.0084	0.0033	0.0012	0.0018

Table 4. Selected MDA and MDA_c values for ⁶⁰Co.

t _s (s)	t _b (s)	MDA _c (eq 3) (Bq cm ⁻²)			
		NaI	18 %	42 %	68 %
1	1	0.24	0.35	0.16	0.11
10	10	0.064	0.05	0.026	0.018
60	60	0.025	0.014	0.0077	0.0056
900	900	0.017	0.0086	0.0050	0.0037
		MDA (eq 2) (Bq cm ⁻²)			
1	∞	0.19	0.33	0.15	0.10
10	∞	0.047	0.043	0.022	0.015
60	∞	0.018	0.011	0.0060	0.0044
900	∞	0.0044	0.0019	0.0012	0.00087

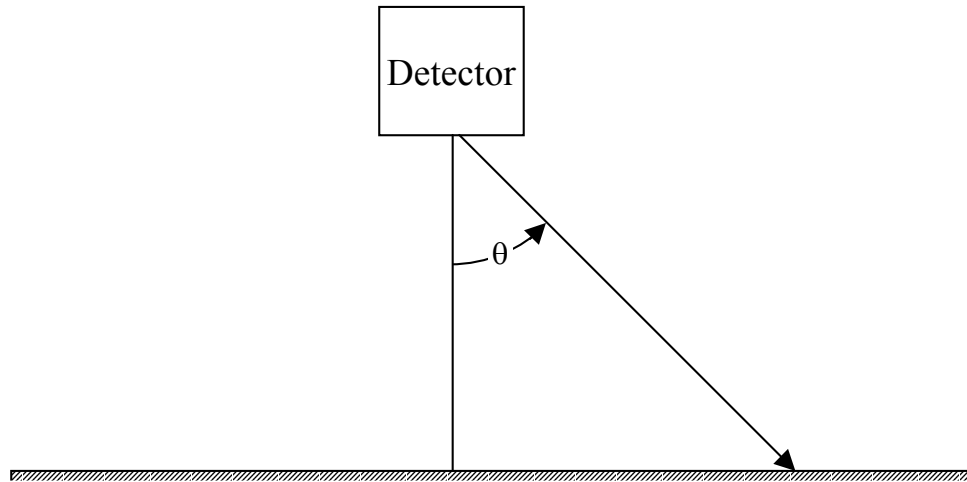


Figure 1. Showing definition of θ , the zenith angle from normal to the ground.

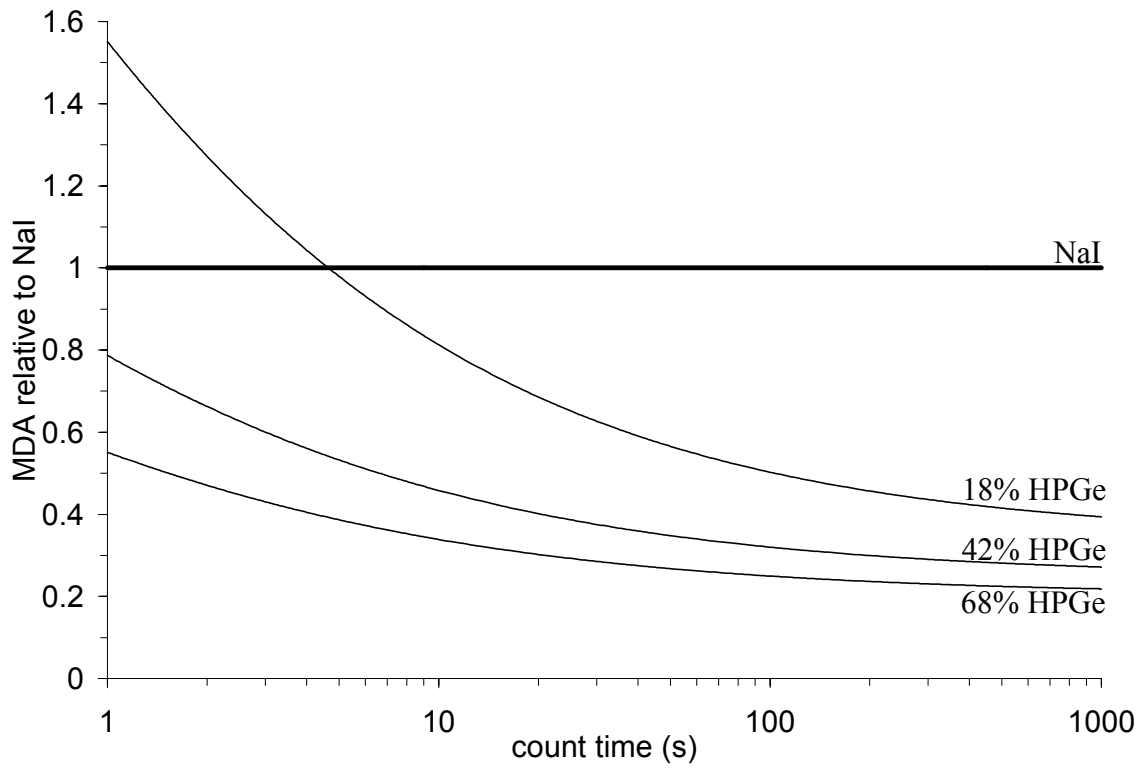


Figure 2. Normalized MDA (eq 2) for ^{137}Cs , in a plane distribution, of a 76mm x 76mm NaI detector and a number of efficiencies of HPGe detectors versus count time under the assumption that the background was collected for significantly longer than the sample.

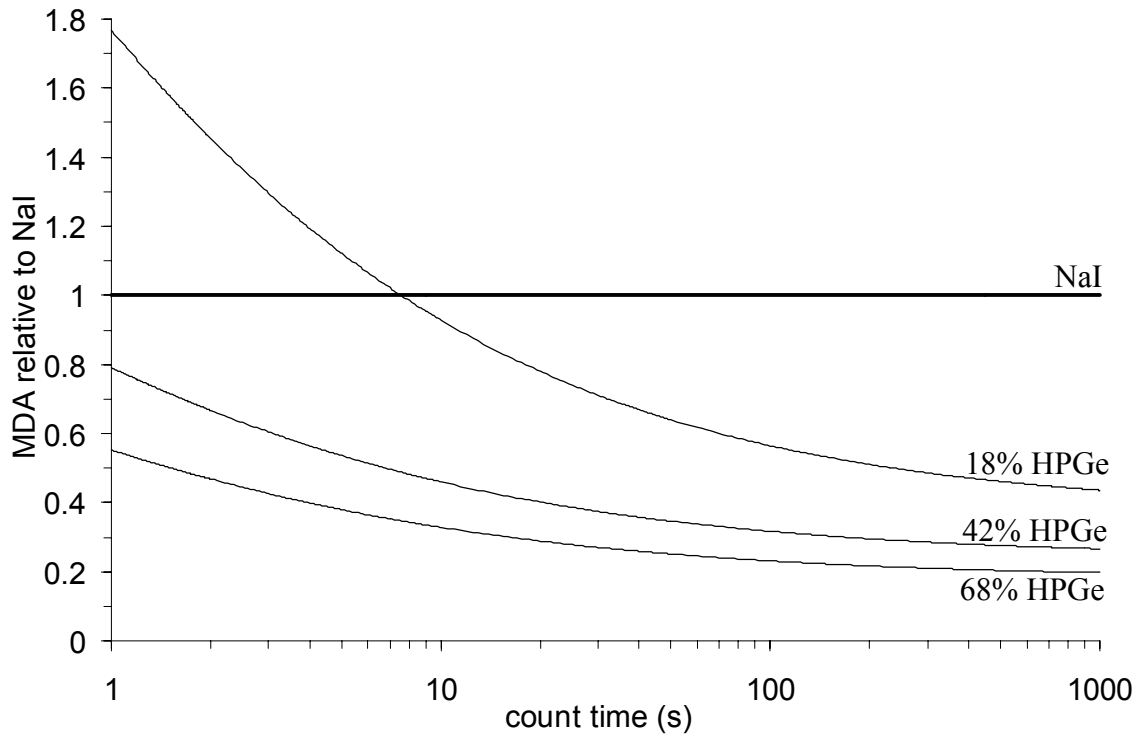


Figure 3. Normalized MDA (eq 2) for ^{60}Co , in a plane distribution, of a 76mm x 76mm NaI detector and a number of efficiencies of HPGe detectors versus count time under the assumption that the background was collected for significantly longer than the sample.

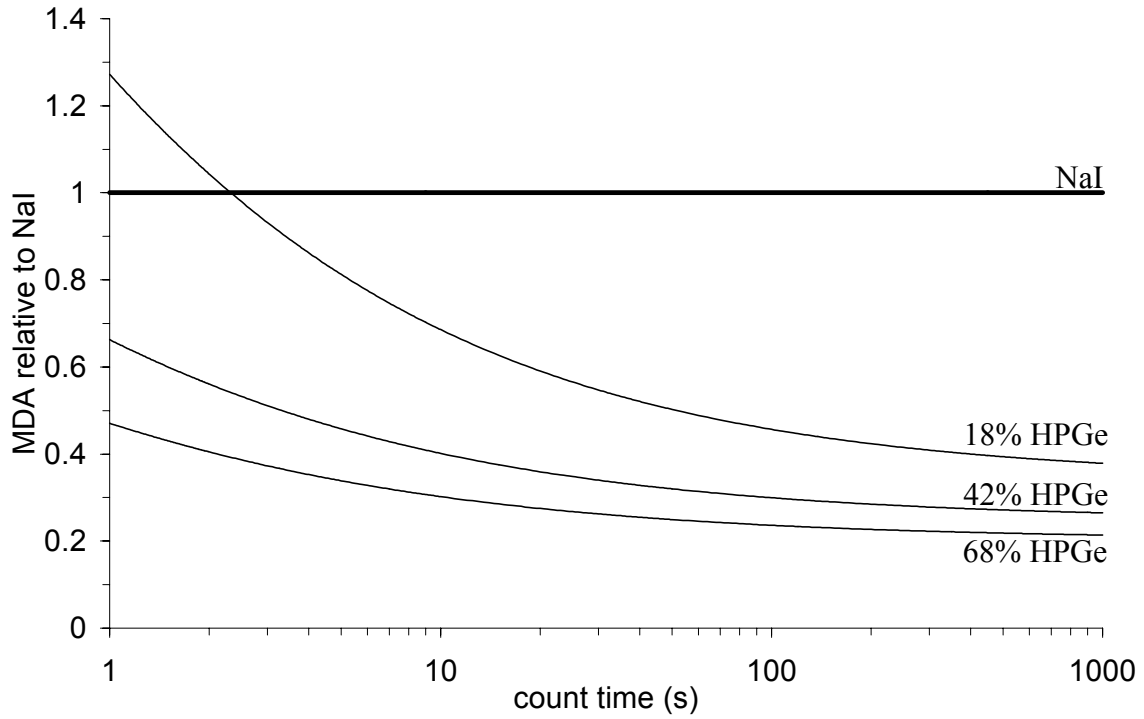


Figure 4. Normalized MDA_c (eq 3) for ^{137}Cs , in a plane distribution, of a 76mm x 76mm NaI detector and a number of efficiencies of HPGe detectors versus count time under conservative assumption that the background was collected for the same amount of time as the sample.

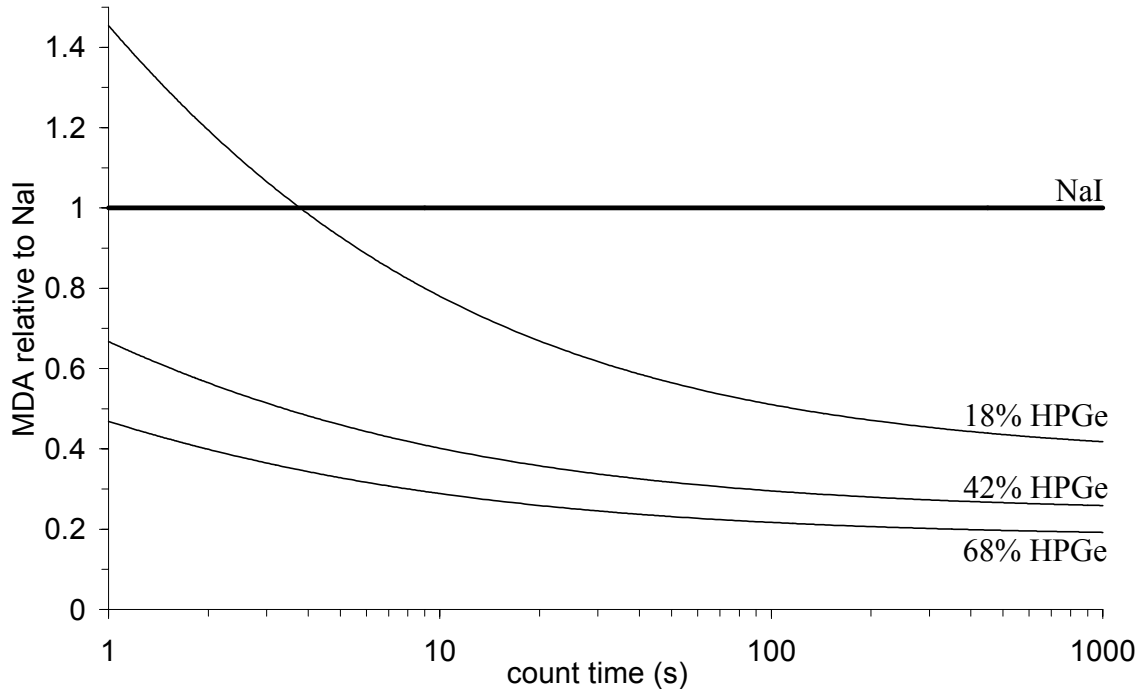


Figure 5. Normalized MDA_c (eq 3) for ^{60}Co , in a plane distribution, of a 76mm x 76mm NaI detector and a number of efficiencies of HPGe detectors versus count time under conservative assumption that the background was collected for the same amount of time as the sample.

APPENDIX A. CALCULATION OF UNCERTAINTY

UNCERTAINTY ON THE EXPOSURE RATE ON THE ROOF OF 201 VARICK STREET.

The equation for gamma-ray exposure rate on the roof of 201 Varick Street is given by

$$X_{roof} = X_{PIC} - X_c$$

where X_{PIC} is the exposure rate as measured by a Pressurized Ionization Chamber (PIC) and X_c is the cosmic radiation contribution.

The absolute standard uncertainty of the non-cosmic exposure rate can be written as

$$\Delta X_{roof} = \sqrt{(\Delta X_{PIC})^2 + (\Delta X_c)^2}$$

The PIC's calibration claims a 5 % relative standard uncertainty, and the cosmic contribution is 3.6 $\mu\text{R/h}$ with a relative standard uncertainty of 0.2 $\mu\text{R/h}$. With the reading at 7.1 $\mu\text{R/h}$, and solving for the relative uncertainty

$$\frac{\Delta X_{roof}}{X_{roof}} = 0.06$$

UNCERTAINTY ON THE BACKGROUND COUNT RATE.

Given the equation for B

$$B \equiv B_{roof} = B_s \cdot c \cdot \frac{X_{roof}}{X_s} \approx B_s \cdot \frac{X_{roof}}{X_s}$$

where c is the correction factor such that $c \cdot X_{roof}/X_s$ is the true correction factor to B_s . This correction factor has an unknown value, near unity. The relative uncertainty of the background count rate can be written as

$$\frac{\Delta B}{B} = \sqrt{\left(\frac{\Delta B_s}{B_s}\right)^2 + \left(\frac{\Delta X_{roof}}{X_{roof}}\right)^2 + \left(\frac{\Delta X_s}{X_s}\right)^2 + \left(\frac{\Delta c}{c}\right)^2}$$

The total number of counts taken is so large that the first term is negligible. The relative uncertainty in X_s will be estimated as uniformly distributed as in the range of -3% to 3% resulting from possible bias in the method. The uncertainty on c can be estimated by recalling that the method cannot move B_s in the wrong direction (i.e. $(c \cdot X_{roof}/X_s)$ and (X_{roof}/X_s) must be on the same side of unity), and by estimating that it would also be impossible for the correction to move B_s as much as twice too far. Thus the value of Δc can be bound using the bound observed value of $\max(\text{abs}(1 - X_{roof}/X_s)) = 0.26$, and taking the relative uncertainty to be triangularly distributed with bounds of -26% to 26% . The value of c is then bound by $c \geq 1 - 0.26 = 0.74$ and substituting these terms in

$$\frac{\Delta B}{B} \leq \sqrt{(0)^2 + (0.06)^2 + \left(\frac{0.06}{\sqrt{3}}\right)^2 + \left(\frac{0.26/\sqrt{6}}{0.74}\right)^2} = 0.21$$

UNCERTAINTY IN THE MINIMUM DETECTABLE ACTIVITY.

Given the equation for the MDA

$$MDA = \frac{3 + 3.27 \cdot \sqrt{B \cdot t_s (1 + t_s/t_b)}}{eff \cdot t_s}$$

assuming that t_s and t_b to have negligible uncertainties, the uncertainty on the MDA can be written as

$$\Delta MDA = \sqrt{\left(\frac{\partial MDA}{\partial B} \Delta B\right)^2 + \left(\frac{\partial MDA}{\partial eff} \Delta eff\right)^2}$$

$$\Delta MDA = \sqrt{\left(\frac{3.27 \cdot t_s (1 + t_s/t_b)}{eff \cdot t_s \cdot 2 \sqrt{B \cdot t_s (1 + t_s/t_b)}} \Delta B\right)^2 + \left(-\frac{3 + 3.27 \cdot \sqrt{B t_s (1 + t_s/t_b)}}{eff^2 \cdot t_s} \cdot \Delta eff\right)^2}$$

$$\Delta MDA = \sqrt{\left(\left(\frac{3 + 3.27 \cdot \sqrt{B t_s (1 + t_s/t_b)}}{\text{eff} \cdot t_s} - \frac{3}{\text{eff} \cdot t_s} \right) \frac{\Delta B}{2B} \right)^2 + \left(MDA \cdot \frac{\Delta \text{eff}}{\text{eff}} \right)^2}$$

$$\Delta MDA = \sqrt{\left(\left(1 - \frac{3}{\text{eff} \cdot t_s \cdot MDA} \right) MDA \cdot \frac{\Delta B}{2B} \right)^2 + \left(MDA \cdot \frac{\Delta \text{eff}}{\text{eff}} \right)^2}$$

$$\Delta MDA = \sqrt{\left(\left(\frac{3.27 \cdot \sqrt{B \cdot t_s (1 + t_s/t_b)}}{3 + 3.27 \cdot \sqrt{B \cdot t_s (1 + t_s/t_b)}} \right) MDA \frac{\Delta B}{2B} \right)^2 + \left(MDA \cdot \frac{\Delta \text{eff}}{\text{eff}} \right)^2}$$

With the relative uncertainty given by

$$\frac{\Delta MDA}{MDA} = \sqrt{\left(\left(\frac{3.27 \cdot \sqrt{B \cdot t_s (1 + t_s/t_b)}}{3 + 3.27 \cdot \sqrt{B \cdot t_s (1 + t_s/t_b)}} \right) \frac{\Delta B}{2B} \right)^2 + \left(\frac{\Delta \text{eff}}{\text{eff}} \right)^2}$$

this can be bound by noticing that

$$\frac{3.27 \cdot \sqrt{B \cdot t_s (1 + t_s/t_b)}}{3 + 3.27 \cdot \sqrt{B \cdot t_s (1 + t_s/t_b)}} \leq 1$$

substituting this in

$$\frac{\Delta MDA}{MDA} \leq \sqrt{\left(\frac{\Delta B}{2B} \right)^2 + \left(\frac{\Delta \text{eff}}{\text{eff}} \right)^2} = 0.12$$

given that the relative standard uncertainty on the efficiency is estimated at 5 % (by calibration documentation).



Environmental Measurements Laboratory
U. S. Department of Energy
201 Varick Street, 5th floor, New York, NY 10014-4811
<http://www.eml.doe.gov>

